A multi-scale vector spline method for estimating the fluids motion on satellite images

Till Isambert, Jean-Paul Berroir, Isabelle Herlin

INSTITUT NATIONAL DE RECHERCHE EN INFORMATIQUE ET EN AUTOMATIQUE

A multi-scale vector spline method for estimating the fluids motion on satellite images

Till Isambert — Jean-Paul Berroir — Isabelle Herlin

N° ????

Mars 2008

Thème NUM

ISSN 0249-6399 ISRN INRIA/RR--????--FR+ENG

A multi-scale vector spline method for estimating the fluids motion on satellite images

Till Isambert , Jean-Paul Berroir , Isabelle Herlin

Thème NUM — Systèmes numériques
Équipe-Projet Clime, commun avec le CEREA, laboratoire joint ENPC - EDF R&D - Université Paris Est

Rapport de recherche n° ???? — Mars 2008 — 14 pages

Abstract: Assessing motion from sequences of atmospheric and oceanographic satellite images is required for environmental simulation, as the dynamic information provided by these images has a strong potential for constraining the models. These images display fluid and potentially turbulent flows. Methods based on vector splines are very efficient to assess motion in this context: they easily allow the conservation law to be taken into account where it is valid and not over the whole image domain; they efficiently implement the 2nd order div-curl regularization, advocated for turbulent fluids, avoiding complex and unstable iterative schemes. The contribution of this paper is to formulate vector splines in a multiscale scheme, with the double objective of assessing motion even in the case of coarse time-sampling and capturing the spectrum of spatial scales associated to turbulent flows. The resulting method only requires the inversion of a band matrix, which is performed by an efficient numerical scheme making the method tractable for large satellite images. Selected results are presented to illustrate the effectiveness of the three characteristics of the approach: the use of control points, 2nd order div-curl regularity, and multiscale formulation.

Key-words: Motion, fluid, multiscale, vector spline, satellite image, 2nd order div-curl regularity

Centre de recherche INRIA Paris – Rocquencourt
Domaine de Voluceau, Rocquencourt, BP 105, 78153 Le Chesnay Cedex
Téléphone : +33 1 39 63 55 11 —Télécopie : +33 1 39 63 53 30

Une méthode de spline vectorielle multi-échelles pour l'estimation du mouvement de fluides à partir d'images satellite

Résumé : L'information dynamique apportée par les images satellite de l'atmosphère et de l'océan a un potentiel important pour contraindre les modèles de simulation environnementale. Ces images visualisent des écoulements fluides et turbulents. Les méthodes de splines vectorielles sont efficaces pour en estimer le mouvement : elles permettent de ne considérer l'équation de conservation que là où elle est valide et non uniformément sur le domaine image ; elles fournissent une implémentation efficace de la régularisation div-rot du second ordre, adaptée aux fluides, sans avoir recours à des schémas de minimisation itératifs. Ce rapport présente la formulation des splines vectorielles dans un cadre multi-échelles, avec un objectif double : permettre l'estimation du mouvement quand l'échantillonage temporel est trop faible, et représenter le spectre d'échelles spatiales associé à la turbulence. La méthode ne requiert que l'inversion d'une matrice bande, effectuée à l'aide d'un schéma numérique efficace même sur des images satellite de grande taille. Les résultats illustrent la pertinence des trois caractéristiques de l'approche : utilisation de points de contrôle, régularité div-rot du second ordre, et formulation multi-échelle.

Mots-clés : Mouvement, fluide, multi-échelle, spline vectorielle, image satellite, régularité div-rot du second ordre

1 Introduction

Forecasting is a key issue in environmental domains such as meteorology, atmospheric chemistry, oceanography, or hydrology. A forecast is performed by operating 3D numerical models describing physical conservation laws: Navier-Stokes equations in meteorology, their Boussinesq approximation in oceanography, etc. Velocity is one of the state variables of these models, describing winds or sea currents. Forecasting requires providing an initial state, and hence an initial value of the motion field. Measurements of the real motion are thus required and ingested into models by means of data assimilation methods [1] to control this initial state. Operational meteorological and oceanographic forecast models make use of in situ observations for this purpose, provided by e.g. ground stations, balloons, drifting buoys.

One of the challenges in environmental modelling is thus the ability to derive motion estimates from dynamic satellite data. The objectives are to complement in situ data in remote or low equipped areas and to improve the spatial resolution of the models' input data. Atmospheric and oceanographic satellite images visualize a 2D turbulent fluid flow, whose link with real 3D motion is non trivial. For instance on meteorological acquisitions in the water vapor band, the pixel value results from contributions of water particles in the vertical column, hence the 2D image motion is a complex combination of real 3D motions at the vertical of the pixel; on infrared data, images visualize the so-called cloud motion wind, i.e. the horizontal displacement of the cloud layers, that has a complex relation with the 3D atmospheric wind. Despite these limitations, image motion fields are considered to be essential data sources for environmental forecast.

Assessing image motion requires setting up an image processing model, defining a 2D conservation law and the required regularity properties to constrain the estimation. These models usually result from a heuristic approach rather than from effective physical properties. State-of-the-art models for fluid flow estimation are characterized by the following three properties. (1) Depending on the acquisition process and fluid nature, the conservation equation applies either to the luminance [2] or to the mass [3, 4]. (2) The regularity is modelled by the 2nd order div-curl constraint, which provides direct control of the Helmholtz decomposition of the motion field in terms of divergence and vorticity [5]. (3) Specific numerical schemes are required in the case of coarse time-sampling, that may prevent the reliable estimation of temporal derivatives. The possible solutions are to formulate motion estimation as a matching problem [6], to integrate the conservation equation over time [7], or to make use of a multiscale scheme [8, 9]. The last solution has the additional advantage of describing the spectrum of spatial scales associated to turbulent flows.

Solving the image processing model is usually addressed by setting up an energy functional made up of two components, one based on the conservation equation to describe confidence in the data, the other using the norm of the motion vector to describe the regularity of the resulting field. This energy must be minimized, for instance by gradient-based approaches or least square methods in the case of parametric motion models, to provide a solution that reaches a compromise between the two components. This approach is unsuitable for application to satellite data for two main reasons. First, the conservation equation can be locally incorrect or unworkable due to missing data, cloud occlusions, 3D phenomena such as upwelling and convection, absence of contrast, or motion

parallel to contours. The conservation law should therefore not be taken into account over the whole image domain. Second, the iterative minimization of the 2nd order div-curl regularity constraint leads to 4th order PDEs, hence to complex and unstable numerical schemes. Neither the convexity of the energy functional nor the convergence to a global minimum can be guaranteed.

An elegant solution to these two problems is provided by spline-based methods [10]. First, they make it possible to easily formulate models in which data confidence applies only at selected locations: the so-called control points. Second, they do not require an iterative energy minimization. Vector-valued thin-plate splines minimize the 2nd order div-curl regularity constraint, and have been proved efficient to interpolate wind measurements provided by ground stations [11]. The use of thin-plate vector splines for image motion estimation has been further proposed by [12], who formulated a vector spline model in which the 2D conservation law is satisfied at control points.

Thin-plate splines are, however, unsuitable for multiscale estimation. A vector spline is defined from a single radial basis function, applied at each control point. A scale-resolved spline must be defined from a basis function providing local information, i.e. the motion field in the vicinity of the associated control point, up to a distance defined from the scale. The basis function must therefore be locally supported or bell-shaped. This condition is not met with thin-plate splines, which are based on a harmonic basis function. This paper presents an innovative multiscale formulation of the vector spline method for motion estimation. It consists in setting up a parametric model suitable for multiscale representation. The vector field is a linear combination of compactly supported radial basis functions, scattered on a regular lattice, whose spatial sampling is defined as the spatial scale. Rather than exactly solving the vector spline image model, the solution is searched for within the parametric space, by solving a sparse and well-conditioned linear system. The motion is computed on a pyramidal representation of images, as the sum of a coarse scale motion and increments from one scale to the immediately finer one.

Results are presented to demonstrate the effectiveness of the characteristics of the multiscale vector spline. A comparison is first made with a gradient-based method that makes use of the same conservation equation and regularity constraint, illustrating the need to apply the conservation equation only at control points. A comparison with methods based on the L^2 regularization is then performed to highlight the suitability of the 2nd order div-curl constraint. The multiscale and single scale splines are finally compared on a strongly turbulent case.

This paper is organized as follows: the vector spline methods for fluid motion estimation are presented in section 2. The main contribution of the paper, multiscale vector splines, is detailed in section 3. Results are analyzed in section 4, and conclusions and prospects for future work are given in section 5.

2 Apparent motion estimation using vector splines

2.1 Interpolation and approximation of vector data

The vector spline model is defined from: (1) a set of n control points $\mathbf{x}_i$ in a spatial domain Ω; (2) vector observations $\mathbf{w}_i$ at these control points. An

interpolating spline is the solution of the following constrained minimization problem:

$$\begin{cases} \min \int_\Omega \|\mathbf{w}\|_d^2 \\ \mathbf{w}(\mathbf{x}_i) = \mathbf{w}_i \ \ \forall i \end{cases} \tag{1}$$

$\|\mathbf{w}\|_d$ denotes the 2nd order div-curl semi-norm, defined as:

$$\|\mathbf{w}\|_d^2 = \alpha \|\nabla \mathrm{div}\, \mathbf{w}\|^2 + \beta \|\nabla \mathrm{curl}\, \mathbf{w}\|^2 \tag{2}$$

It is a semi-norm since its nullity does not imply that the vector field is 0: actually, the zero-space of the 2nd order div-curl norm is the set of affine vector fields. This minimization problem admits a unique solution (the demonstration is given in [11]), a thin-plate spline based on the harmonic radial basis function ϕ solution of $\Delta^3 \phi = \delta$ (δ being the Dirac function):

$$\phi(\mathbf{x}) = (128\pi)^{-1} \|\mathbf{x}\|^4 \log \|\mathbf{x}\| \tag{3}$$

The solution of the minimization problem (1) is the field $\mathbf{w} = (u, v)$ defined as:

$$u = p(\mathbf{x}) + \sum_{i=1}^{n} a_i \left(\frac{1}{\alpha} \phi_{xx}(\mathbf{x} - \mathbf{x}_i) + \frac{1}{\beta} \phi_{yy}(\mathbf{x} - \mathbf{x}_i) \right) + b_i \left(\frac{1}{\alpha} - \frac{1}{\beta} \right) \phi_{xy}(\mathbf{x} - \mathbf{x}_i) \tag{4}$$

$$v = q(\mathbf{x}) + \sum_{i=1}^{n} a_i \left(\frac{1}{\alpha} - \frac{1}{\beta} \right) \phi_{xy}(\mathbf{x} - \mathbf{x}_i) + b_i \left(\frac{1}{\alpha} \phi_{yy}(\mathbf{x} - \mathbf{x}_i) + \frac{1}{\beta} \phi_{xx}(\mathbf{x} - \mathbf{x}_i) \right) \tag{5}$$

p and q are polynomials of degree 1 ($p(\mathbf{x}) = c_1 + c_2 x + c_3 y$, $q(\mathbf{x}) = d_1 + d_2 x + d_3 y$). $\mathbf{a} = (a_i)$, $\mathbf{b} = (b_i)$, $\mathbf{c} = (c_i)$ and $\mathbf{d} = (d_i)$ are real coefficients whose values are obtained by setting the interpolation condition $\mathbf{w}(\mathbf{x}_i) = \mathbf{w}_i^{obs}$, $i = 1, \ldots, n$:

$$\begin{pmatrix} Q & S \\ S^T & 0 \end{pmatrix} \begin{pmatrix} \mathbf{a} \\ \mathbf{b} \\ \mathbf{c} \\ \mathbf{d} \end{pmatrix} = \begin{pmatrix} \mathbf{w}^{obs} \\ 0 \end{pmatrix} \tag{6}$$

$\mathbf{w}^{obs}$ denotes the $2n$ vector of observations at control points, the matrices Q ($2n \times 2n$) and S ($2n \times 6$) are defined by:

$$Q = \frac{1}{\alpha} \begin{pmatrix} \phi_{xx}(\mathbf{x} - \mathbf{x}_i) & \phi_{xy}(\mathbf{x} - \mathbf{x}_i) \\ \phi_{xy}(\mathbf{x} - \mathbf{x}_i) & \phi_{yy}(\mathbf{x} - \mathbf{x}_i) \end{pmatrix} + \frac{1}{\beta} \begin{pmatrix} \phi_{yy}(\mathbf{x} - \mathbf{x}_i) & -\phi_{xy}(\mathbf{x} - \mathbf{x}_i) \\ -\phi_{xy}(\mathbf{x} - \mathbf{x}_i) & \phi_{xx}(\mathbf{x} - \mathbf{x}_i) \end{pmatrix} \tag{7}$$

and:

$$S = \begin{pmatrix} \begin{pmatrix} 1 & x_1 & y_1 \\ \vdots & \vdots & \vdots \\ 1 & x_n & y_n \end{pmatrix} & 0 \\ 0 & \begin{pmatrix} 1 & x_1 & y_1 \\ \vdots & \vdots & \vdots \\ 1 & x_n & y_n \end{pmatrix} \end{pmatrix} \tag{8}$$

An approximating spline is defined as the solution of the following minimization problem:

$$\min \left\{ \sum_i (\mathbf{w}(\mathbf{x}_i) - \mathbf{w}_i)^2 + \lambda \int_\Omega \|\mathbf{w}\|_d^2 \right\} \tag{9}$$

where the parameter λ controls the compromise between confidence in the data and regularity. This spline has the same generic expression (eqs 4 and 5) as the interpolating spline. Its coefficients $\mathbf{a}$, $\mathbf{b}$, $\mathbf{c}$ and $\mathbf{d}$ are obtained by solving:

$$\begin{pmatrix} Q + \lambda Id & S \\ S^T & 0 \end{pmatrix} \begin{pmatrix} \mathbf{a} \\ \mathbf{b} \\ \mathbf{c} \\ \mathbf{d} \end{pmatrix} = \begin{pmatrix} \mathbf{w}^{obs} \\ 0 \end{pmatrix} \tag{10}$$

The computation time is the same for the interpolating and approximating splines. A $(2n+6) \times (2n+6)$ -dense- linear system must be inverted to get the vectors $\mathbf{a}$ to $\mathbf{d}$. The spline is then computed at every location $\mathbf{x}$ using equations (4) and (5). This requires computing, for each location $\mathbf{x}$, the partial derivatives of ϕ at $\mathbf{x} - \mathbf{x}_i$, $\mathbf{x}_i$ spanning the control points. As ϕ is not bell-shaped, there is no possibility of speeding up the computation by discarding remote control points where ϕ vanishes. The only user-defined coefficients of the vector spline model are α and β, which control the variations of divergence and curl of the field, and, in the case of the approximating spline, λ, which controls the compromise between confidence in the data and regularity.

2.2 Motion estimation using vector splines

The use of vector splines for motion estimation from image data has been proposed in [12] for the case of the luminance conservation equation, and in [13] for mass conservation. In contrast to the previous formulation, no vector observations are available, but an indirect observation is provided by the conservation equation. The latter is formulated as: $\mathcal{L}\mathbf{w} + I_t = 0$, $\mathcal{L}$ being a linear observation operator. If assuming luminance conservation, we have $\mathcal{L}\mathbf{w} = \nabla I.\mathbf{w}$, and if assuming mass conservation: $\mathcal{L}\mathbf{w} = (\nabla I + I\nabla).\mathbf{w}$. For both cases, at each control point $\mathbf{x}_i$, we have $\mathcal{L}_i.\mathbf{w} = -I_t$, $\mathcal{L}_i$ denoting the observation operator at control point $\mathbf{x}_i$.

The vector spline model can be rewritten as:

$$\left\{ \begin{array}{l} \min \displaystyle\int_\Omega \|\mathbf{w}\|_d^2 \\ \mathcal{L}_i\mathbf{w} + I_t = 0 \end{array} \right. \quad \text{or:} \quad \min \left\{ \sum_i (\mathcal{L}_i\mathbf{w} + I_t)^2 + \lambda \int_\Omega \|\mathbf{w}\|_d^2 \right\} \tag{11}$$

for the interpolation and approximation cases. It can be proven that the solution of (11) exists and is unique if the observation operators $\mathcal{L}_i$ are linear and non zero, and if the control points are non aligned. This solution is a thin-plate spline, with the same basis function ϕ as in subsection 2.1:

$$\mathbf{w} = \sum_{i=1}^{n} c_i \mathcal{L}_i \phi(\|\mathbf{x} - \mathbf{x}_i\|) + \sum_{i=1}^{6} d_i p_i(\mathbf{x}) \tag{12}$$

$\mathbf{p} = (p_i)$ being a basis of degree 1 polynomials. The vectors of coefficients $\mathbf{c} = (c_i)$ and $\mathbf{d} = (d_i)$ are solution of:

$$\begin{pmatrix} Q + \lambda Id & S \\ S^T & 0 \end{pmatrix} \begin{pmatrix} \mathbf{c} \\ \mathbf{d} \end{pmatrix} = \begin{pmatrix} -It \\ 0 \end{pmatrix} \tag{13}$$

The general term of Q $(n \times n)$ is $\mathcal{L}_i \mathcal{L}_j \phi(\|\mathbf{x}_i - \mathbf{x}_j\|)$ and S $(n \times 6)$ is defined as: $S = \mathcal{L}_i \mathbf{p}$.

The vector spline model used for image motion estimation shares the same interesting properties as the model used for interpolating or approximating vector data: its solution is directly obtained without iterative minimization, and it has few parameters (i.e. α, β and λ). One will set $\alpha \gg \beta$ when processing images of highly turbulent flows, thus favoring an estimation with large curl variability. Reversely, $\beta \gg \alpha$ is appropriate for situations such as intense vertical activity causing locally divergent flows.

One main difference with vector data is that there are no predefined locations where motion observations are available. A control point selection process must be implemented prior to the estimation. The theoretical conditions guaranteeing the existence and uniqueness of the solution can easily be met by selecting these control points with a double thresholding: first on the magnitude of the spatial gradient, discarding low contrast areas; second on the magnitude of the motion index, thus discarding visually still areas. Depending on the environmental domain, further locations in specific structures must be discarded. This is, for instance, the case of ejection filaments in oceanography, as in these structures the motion is parallel to the contours and the conservation equation is degenerated. The selection of control points is therefore highly application-dependent; they should be as evenly distributed as possible, but there is, to our knowledge, no criterion for defining an optimal distribution of control points.

3 Multiscale vector splines

3.1 Parametric spline model

Thin-plate vector splines minimize the 2nd order div curl regularity, but are inappropriate for multiscale estimation as they are defined from a harmonic basis function. A multiscale scheme actually requires using a basis function that provides a local representation of motion, hence locally supported or rapidly decaying. The contribution of this paper is to formulate a multiscale spline model, based on a parametric spline used for each scale and on a pyramidal representation of images at different scales.

We consider the spline approximation problem with the 2nd order div-curl norm and either the luminance or the mass conservation equation, through the observation operators $\mathcal{L}_i$ assessed on the n control points $\mathbf{x}_i$:

$$\min J(\mathbf{w}) = \left\{ \sum_{i=1}^{n} (\mathcal{L}_i \mathbf{w} - \mathbf{w}_i)^2 + \lambda \int_\Omega \alpha \|\nabla \mathrm{div}\, \mathbf{w}\|^2 + \beta \|\nabla \mathrm{curl}\, \mathbf{w}\|^2 \right\} \tag{14}$$

Rather than exactly solving equation (14), which would lead to a thin-plate spline, the minimum is searched for among a set of spline functions suitable for the multiscale formalism, satisfying the following properties. (1) The spline is

defined from a unique bell-shaped radial basis function of unit support. The choice of this function is not critical as long as it is sufficiently smooth (at least three times continuously differentiable in order to compute the 2nd order div-curl semi-norm). We make use of the basis function ψ proposed by [14] and defined as $\psi(r) = (1-r)^6(35r^2+18r+3)$ for $|r| \leq 1$. (2) The spline is a linear combination of translates of the basis function over a regular lattice of m grid points, whose sampling defines the scale parameter h. The translates of the basis function are dilated by a factor γ proportional to h. The parameters defining the spline are the m weights $\mathbf{q} = (\mathbf{q}_j)$ (each weight $\mathbf{q}_j$ being homogeneous to a motion vector with u and v components) applied to the translates of the basis function. The parametric expression of the vector spline is thus:

$$\mathbf{w}_{\mathbf{q},h}(x) = \sum_{\mathbf{v}_j \in \mathbb{Z}^2, h\mathbf{v}_j \in \Omega} \mathbf{q}_j \psi(\| \frac{\mathbf{x} - h\mathbf{v}_j}{\gamma} \|) \tag{15}$$

where $\mathbf{v}_j$ spans a regular lattice of unit spacing in the image domain Ω.

A new expression of the functional J is defined by substituting, in equation (14), $\mathbf{w}$ by its parametric form $\mathbf{w}_{\mathbf{q},h}$ (15). Let us first consider the first term of J. If the observation operator is based on the luminance conservation equation, its new expression is:

$$\|\mathbf{I_x}\Psi\mathbf{q^u} + \mathbf{I_y}\Psi\mathbf{q^v} - \mathbf{I_t}\|^2 = \|A_l\mathbf{q} - \mathbf{I_t}\|^2 \tag{16}$$

$\mathbf{I_t}$ being the n-dimensional vector of the temporal derivatives at the control points; Ψ being the $n \times m$ matrix of general term $\psi((x_i - k_j)/\gamma, (y_i - l_j)/\gamma)$ with i indexing the n control points and j the m grid points (k,l); $\mathbf{I_x}$ and $\mathbf{I_y}$ are the $n \times n$ diagonal matrices of the image spatial derivatives at the control points. In the case of mass conservation, the first term of J becomes:

$$\|\mathbf{I_x}\Psi\mathbf{q^u} + \mathbf{I_y}\Psi\mathbf{q^v} + \mathbf{I}\mathbf{D_x}\Psi + \mathbf{I}\mathbf{D_y}\Psi - \mathbf{I_t}\|^2 = \|A_m\mathbf{q} - \mathbf{I_t}\|^2 \tag{17}$$

where $\mathbf{I}$ is the $n \times n$ diagonal matrix formed by the image values at control points, $\mathbf{D_x}\Psi$ and $\mathbf{D_y}\Psi$ are the matrices of the spatial derivatives of Ψ. Whatever the considered conservation equation, the first term of J is rewritten as a quadratic function of $\mathbf{q}$.

Let us now analyze the second term of J. It is first written in a matrix form by introducing the matrix of differential operators $Q(D)$:

$$Q(D) = \begin{pmatrix} \sqrt{\alpha}\partial_{xx} + \sqrt{\beta}\partial_{yy} & (\sqrt{\alpha} - \sqrt{\beta})\partial_{xy} \\ (\sqrt{\alpha} - \sqrt{\beta})\partial_{xy} & \sqrt{\alpha}\partial_{yy} + \sqrt{\beta}\partial_{xx} \end{pmatrix}. \tag{18}$$

then factorized as:

$$\alpha \int \|\nabla \mathrm{div}\, \mathbf{w}\|^2 + \beta \int \|\nabla \mathrm{curl}\, \mathbf{w}\|^2 = \int \|Q(D)\mathbf{w}\|^2 \tag{19}$$

The second term of J is finally rewritten as the quadratic expression $\|R\mathbf{q}\|^2$, with:

$$R = \begin{pmatrix} \sqrt{\alpha}\partial_{xx}\Psi + \sqrt{\beta}\partial_{yy}\Psi & (\sqrt{\alpha} - \sqrt{\beta})\partial_{xy}\Psi \\ (\sqrt{\alpha} - \sqrt{\beta})\partial_{xy}\Psi & \sqrt{\alpha}\partial_{yy} + \sqrt{\beta}\partial_{xx}\Psi \end{pmatrix}. \tag{20}$$

The substitution of $\mathbf{w}$ by the parametric expression $\mathbf{w}_{\mathbf{q},h}$ allows J to be rewritten as a quadratic function of $\mathbf{q}$:

$$J(\mathbf{q}) = \|A\mathbf{q} - I_t\|^2 + \lambda\|R\mathbf{q}\|^2 \tag{21}$$

with A being either A_l or A_m depending on the conservation equation chosen. Finding the minimum of J with respect to $\mathbf{q}$ is now a linear optimization problem!

3.2 Numerical solving

The matrices A and R, in (21), have a band structure since ψ has a compact support of size γ. The width of the band depends on the ratio of γ to the scale parameter h. If γ is small compared to h, the matrices A and R are diagonal, but the vector spline is zero everywhere except in the vicinity of the grid points. If γ is large compared to h, the resulting vector spline can accurately approximate the thin-plate spline, but the A and R matrices are dense and require a heavy computational load. $\gamma = 3h$ has been empirically chosen as a good compromise between the computational speed and the accuracy of the spline. The band structure allows an efficient numerical solving to be implemented. Let $\mathbf{B} = \left(A^TA + \lambda R^TR\right)$ and $\mathbf{d} = -A^TA.I_t$. The problem (21) admits a unique solution $\mathbf{q}$, satisfying the following overconstrained system:

$$\mathbf{Bq} = \mathbf{d}. \tag{22}$$

The solution is computed using a Jacobi pre-conditioning technique [15]. Letting $\tilde{\mathbf{B}} = \mathbf{P}^{-1}\mathbf{BP}$ and $\mathbf{P} = \sqrt{\text{diag}(\mathbf{B})}$, the system is solved in two steps:

$$\tilde{\mathbf{B}}\mathbf{y} = \mathbf{P}^{-1}\mathbf{d} \tag{23}$$

$$\mathbf{q} = \mathbf{P}^{-1}\mathbf{y}, \tag{24}$$

This technique speeds up the computation by taking advantage of the band structure of the matrix $\mathbf{B}$, and introducing the matrix $\mathbf{P}$ further improves the conditioning of the linear system.

3.3 Hierarchical motion estimation

A multiscale scheme is required for two main reasons. (1) The parametric spline allows the image motion to be assessed given a spatial scale parameter h, and provided that the conservation equation can be computed. On satellite image sequences, the time sampling is often too coarse to reliably assess the temporal derivatives of the quickest structures and the conservation equation cannot be computed on the full resolution image. (2) Turbulent flows are associated with a large spectrum of spatial and temporal scales. These two reasons motivate the use of a pyramidal multiscale scheme, in which motion is hierachically computed from the coarsest to the finest scale.

Let I_0 and I_1 be two successive images of the sequence. Both are represented using a pyramid, from the full resolution $I_0(0)$ and $I_1(0)$ to the coarsest scale $I_0(p_{max})$ and $I_1(p_{max})$. To each scale index p corresponds a scale parameter $h(p)$. The motion is initially computed at the coarsest scale with the parametric spline at scale $h(p_{max})$, yielding the motion field $\mathbf{w}(p_{max})$, and then progressively refined by:

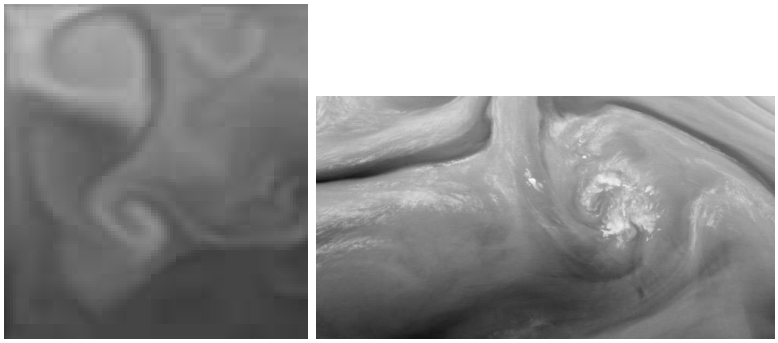

Figure 1: Extract of the test sequences: left, OPA; right: Meteosat.

1. Oversampling $\mathbf{w}(p+1)$ so that it matches the resolution of scale $h(p)$;
2. Compensating image $I_0(p)$ with $\mathbf{w}(p+1)$, yielding the compensated image $I'_0(p)$.
3. Estimating the motion at scale $h(p)$ between $I'_0(p)$ and $I_1(p)$, yielding the motion increment $\delta\mathbf{w}(p)$.

The finest scale motion ($p = 0$) is thus expressed as the sum of a coarse scale motion $\mathbf{w}(p_{max})$ and of increments describing the finer resolutions:

$$\mathbf{w}(0) = \mathbf{w}(p_{max}) + \sum_{p=p_{max}-1}^{0} \delta\mathbf{w}(p) \tag{25}$$

The link between the scale parameter $h(p)$ and the real spatial scale of the evolving image structures is not obvious. At one level of the pyramid, the motion is computed using a scale parameter h corresponding to a basis function of support $\gamma = 3h$. The basis function is thus able to represent motion patterns with spatial size less than $3h$; but there is no guarantee that all motion patterns of that size will be represented: this will occur only if enough control points have been selected in the pattern considered.

4 Results

Comparisons of motion estimates are presented to demonstrate the effectiveness of the three main characteristics of the multiscale spline: the use of the conservation equation only at selected control points; the regularity modelled with the 2nd order div-curl norm; and the use of a pyramidal multiscale scheme.

The first comparison is intended to demonstrate the efficiency of accounting for the conservation only at control points. For this purpose, the motion is computed on Meteosat-5[1] images acquired in the water vapor band (displayed on the right in figure 1). Control points have been automatically selected in areas where the mass conservation equation is not degenerated by thresholding the norm of the spatial gradient and the motion index. The motion is then computed

[1]Copyright Eumetsat

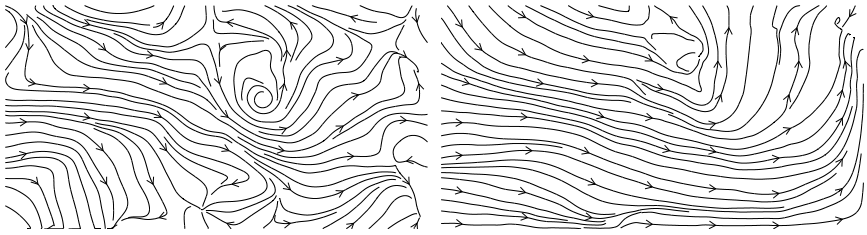

Figure 2: Motion fields estimated on the Meteosat sequence. Left: multiscale spline, right: Corpetti and Mémin.

using the multiscale vector spline. The results are compared to those obtained using Corpetti's method, which uses the same conservation equation and the same regularity constraint, but minimizes a data confidence term evaluated over the whole domain. The results are displayed in figure 2, which renders the motion fields as streamlines, allowing vortices to be visualized as the centres of concentric lines. The multiscale spline is more accurate with respect to the location of the central vortex. It furthermore succeeds in capturing a rotating motion in the lower left part of the image, whereas Corpetti's method incorrectly computes a smooth laminar field.

The second comparison is intended to demonstrate that the 2nd order div-curl regularity must be used for fluid motion assessment. It is computed on the synthetic 'OPA' sequence (on the left in figure 1), obtained by numerical simulation with the OPA ocean circulation model[2]. The OPA sequence provides temperature, used for computing motion, and surface currents, used as the reference field for validation purposes. Figure 3 displays the reference field, the fields obtained by the multiscale spline, by the thin-plate spline, and by the Horn and Schunck method (luminance conservation equation, L^2 regularity). Quantitative criteria suggest that vector spline methods, either thin-plate or the proposed multiscale spline, are more accurate than the method based on L^2 regularity: the mean angular error with the reference is (in degrees) 28 for the multiscale spline, 33 for the thin-plate spline, and 50 for the Horn and Schunck field. Spline methods are much more efficient as far as the detected location of eddies is concerned: only one is located by the Horn and Schunck's method, the remaining part of the flow being almost laminar: this is a consequence of the L^2 regularization, which favors laminar fields. In contrast, the main eddies are correctly located by the spline methods, ran with the α and β parameters tuned to favor the assessment of a motion field with a strongly variable curl.

Figure 4 displays the motion fields estimated on the OPA sequence at three different scales. At the coarsest scale, the main vortices appear in the upper part of the image, and the large vortex in the bottom part is not detected at all. At the intermediate scale, all vortices appear. Their location is then only slightly improved at the finest resolution. This illustrates that the multiscale scheme actually links the size of the spatial structure with the spatial scale of the spline, although this link is not easy to interpret. No comparison is provided to demonstrate that the pyramidal representation is efficient in the case of too coarse a time sampling, as this is now a classical result. The results displayed

[2]Thanks to Marina Levy, LOCEAN, IPSL, France

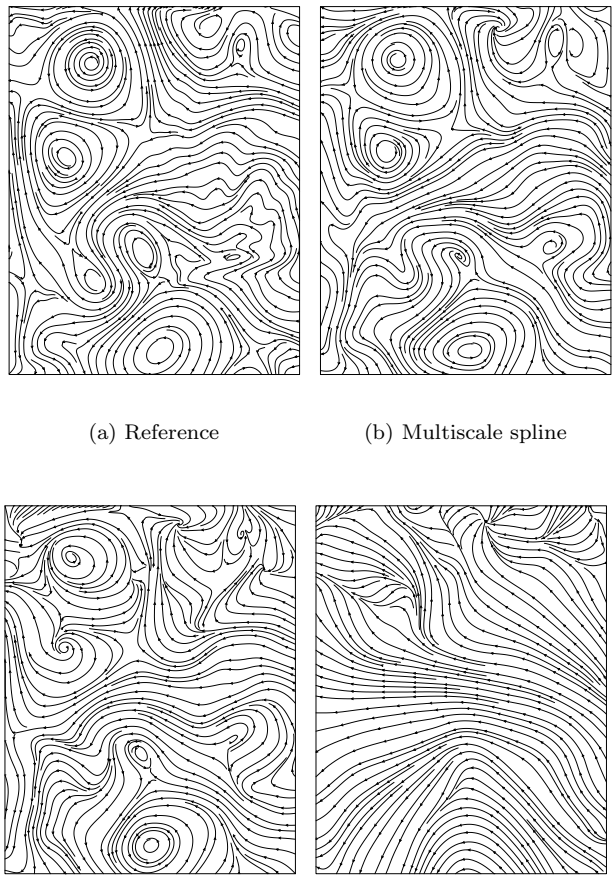

(a) Reference (b) Multiscale spline

(c) Thin-plate spline (d) Horn and Schunk

Figure 3: Comparison of methods on the OPA sequence. The vector splines have been computed using the luminance conservation, $\lambda = 0.1$, $\alpha = 0.9$ and $\beta = 0.1$.

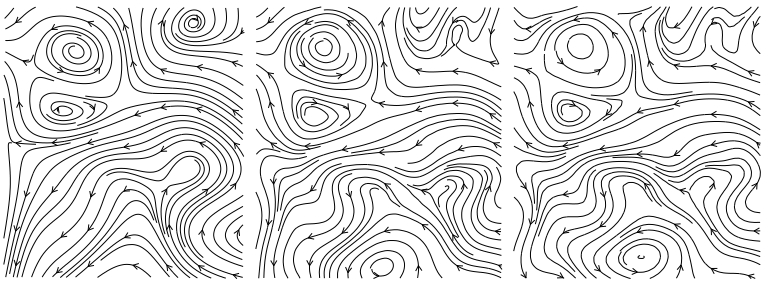

Figure 4: Motion field estimated on the OPA sequence, from the coarsest to the finest (full) resolution.

in figure 2 are obtained on a sequence with a very fast jet motion; however the two methods compared are both using a multiscale scheme.

5 Conclusion and future work

This paper proposes an innovative approach for assessing motion on atmospheric or oceanographic satellite image sequences, displaying fluid and potentially turbulent flows. The characteristics of the approach are the following. (1) The data confidence component of the model is only taken into account at specific locations, the control points, where the conservation equation is valid. This issue is fundamental as suggested by the comparison made with a method using the same conservation equation and the same regularity constraint but solving the conservation equation over the whole image domain. (2) The regularity of the motion field is controlled by the 2nd order div curl constraint. This constraint is appropriate for fluid and turbulent flows, as it allows the variations of divergence and vorticity to be controlled. This is highlighted by comparisons with methods based on L^2 regularization, which are unable to correctly assess the motion field in eddies. (3) A multiscale scheme is adopted to characterize the spectrum of spatial scales related to turbulence, and to allow estimation even in the case of too coarse a time sampling.

Being based on control points and on the 2nd order div curl constraint, the motion field should theoretically be expressed by a thin-plate spline. The theoretical contribution of this paper is to formulate a vector spline in a multiscale scheme, using a parametric spline model. This approach has two main advantages: (1) the minimum of the energy is obtained by solving a linear system; (2) the matrix to invert has a band structure, allowing an efficient implementation that makes the method affordable even for sequences of large images.

The approach requires further investigation on two issues. First, what is the link between the spatial scale of basis functions and the extent of image structures such as vortices? There is no obvious link according to the results and we believe that the control points must also be hierarchically organized for that purpose. Second, it is well known that spatial and temporal scales of turbulent flows are strongly linked, large vortices being stabler that smaller ones. It is thus necessary to consider motion estimation not only from a pair of successive images, but from a longer sequence in order to establish a multiscale representation both in space and time.

References

[1] Korotaev, G., Huot, E., Le Dimet, F.X., Herlin, I., Stanichny, S., Solovyev, D., Wu, L.: Retrieving Ocean Surface Current by 4D Variational Assimilation of Sea Surface Temperature Images. Remote Sensing of Environment (2007) Special Issue on Data Assimilation.

[2] Horn, B., Schunck, B.: Determining optical flow. AI **17** (1981) 185–203

[3] Béréziat, D., Herlin, I., Younes, L.: A generalized optical flow constraint and its physical interpretation. In: Proceedings of Computer Vision and Pattern Recognition, Hilton Head Island, USA, IEEE (2000) 487–492

[4] Wildes, R., Amabile, M.: Physically based fluid flow recovery from image sequences. In: Computer Vision Pattern Recognition, Puerto Rico (1997) 969–975

[5] Gupta, S., Princ, J.: Stochastic models for div-curl optical flow methods. IEEE Signal Processing Letter **3** (1996)

[6] Bouthemy, P., Benveniste, A.: Modeling of atmospheric disturbances in meteorological pictures. IEEE Trans. on Pattern Analysis and Machine Intelligence **6** (1984) 587–600

[7] Corpetti, T., Memin, E., Perez, P.: Dense estimation of fluid flows. PAMI **24** (2002) 365–380

[8] Horn, U., Girod, B.: Performance analysis of multiscale motion compensation techniques in pyramid coders (1996)

[9] Moulin, P., Krishnamurthy, R., Woods, J.: Multiscale modeling and estimation of motion fields for video coding (1997)

[10] Duchon, J.: Splines minimizing rotation-invariant semi-norms in Sobolev spaces. Lecture notes in mathematics, constructive theory of functions of several variables **571** (1976) 85–100

[11] Amodei, L.: A vector spline approximation. Journal of approximation theory **67** (1991) 51–79

[12] Suter, D.: Motion estimation and vector splines. In: CVPR94. (1994)

[13] Isambert, T., Herlin, I., Berroir, J., Huot, E.: Apparent motion estimation for turbulent flows with vector spline interpolation. In: XVII IMACS world congress, Scientific Computation Applied Mathematics and Simulation, Paris, July, 11-15. (2005)

[14] Wendland, H.: Piecewise polynomial, positive definite and compactly supported radial basis functions of minimal degree. Advances in Computational Mathematics **4** (1995) 389–396

[15] Fasshauer, G.: Solving differential equations with radial basis functions: multilevel methods and smoothing. Advances in Computational Mathematics **11** (1999) 139–159

Centre de recherche INRIA Paris – Rocquencourt
Domaine de Voluceau - Rocquencourt - BP 105 - 78153 Le Chesnay Cedex (France)

Centre de recherche INRIA Bordeaux – Sud Ouest : Domaine Universitaire - 351, cours de la Libération - 33405 Talence Cedex
Centre de recherche INRIA Grenoble – Rhône-Alpes : 655, avenue de l'Europe - 38334 Montbonnot Saint-Ismier
Centre de recherche INRIA Lille – Nord Europe : Parc Scientifique de la Haute Borne - 40, avenue Halley - 59650 Villeneuve d'Ascq
Centre de recherche INRIA Nancy – Grand Est : LORIA, Technopôle de Nancy-Brabois - Campus scientifique
615, rue du Jardin Botanique - BP 101 - 54602 Villers-lès-Nancy Cedex
Centre de recherche INRIA Rennes – Bretagne Atlantique : IRISA, Campus universitaire de Beaulieu - 35042 Rennes Cedex
Centre de recherche INRIA Saclay – Île-de-France : Parc Orsay Université - ZAC des Vignes : 4, rue Jacques Monod - 91893 Orsay Cedex
Centre de recherche INRIA Sophia Antipolis – Méditerranée : 2004, route des Lucioles - BP 93 - 06902 Sophia Antipolis Cedex

Éditeur
INRIA - Domaine de Voluceau - Rocquencourt, BP 105 - 78153 Le Chesnay Cedex (France)
http://www.inria.fr
ISSN 0249-6399